

Transverse dimensions of chorus in the source region

O. Santolík¹ and D. A. Gurnett

Department of Physics and Astronomy, University of Iowa, Iowa City, USA

Received 27 August 2002; revised 12 October 2002; accepted 30 October 2002; published 16 January 2003.

[1] We report measurement of whistler-mode chorus by the four Cluster spacecraft at close separations. We focus our analysis on the generation region close to the magnetic equatorial plane at a radial distance of 4.4 Earth's radii. We use both linear and rank correlation analysis to define perpendicular dimensions of the sources of chorus elements below one half of the electron cyclotron frequency. Correlation is significant throughout the range of separation distances of 60–260 km parallel to the field line and 7–100 km in the perpendicular plane. At these scales, the correlation coefficient is independent for parallel separations, and decreases with perpendicular separation. The observations are consistent with a statistical model of the source region assuming individual sources as gaussian peaks of radiated power with a common half-width of 35 km perpendicular to the magnetic field. This characteristic scale is comparable to the wavelength of observed waves.

INDEX TERMS: 2772 Magnetospheric Physics: Plasma waves and instabilities; 2730 Magnetospheric Physics: Magnetosphere—inner; 6939 Radio Science: Magnetospheric physics; 6984 Radio Science: Waves in plasma; 2778 Magnetospheric Physics: Ring current.
Citation: Santolík, O., and D. A. Gurnett, Transverse dimensions of chorus in the source region, *Geophys. Res. Lett.*, 30(2), 1031, doi:10.1029/2002GL016178, 2003.

1. Introduction

[2] Emissions of electromagnetic waves in the Earth's magnetosphere known as chorus are characterized by a sequence of discrete elements appearing as intense short-duration (typically 10^{-1} s) rising, or, less often, falling tones in the frequency range from a few hundreds of hertz to several kHz (see, e.g., reviews by *Omura et al.*, [1991] or *Sazhin and Hayakawa* [1992]). Although it is generally accepted that their generation is connected with the electron cyclotron resonance of whistler-mode waves and radiation belt electrons [*Helliwell*, 1967], the properties of the chorus source are still a subject of active experimental and theoretical research [e.g., *Lauben et al.*, 1998; *LeDocq et al.*, 1998; *Trakhtengerts*, 1999; *Gurnett et al.*, 2001]. The size of the interaction region is one of the parameters which can allow us to compare theoretical predictions with the observations. *Helliwell* [1967] predicted the length of the source parallel to the field line as a function of the wave frequency and parameters of the plasma medium; if a source is localized close to the magnetic equatorial plane at radial

distances of 4 Earth's radii (R_E), and if it emits waves at frequencies below one half on the electron cyclotron frequency ($\frac{1}{2}f_{ce}$) then its parallel dimension should be of the order of 1000–3000 km, depending on the plasma density. More recently, *Trakhtengerts* [1999] proposed that, close to the equatorial plane, a characteristic scale of spatial features (localizations) of chorus generation should be approximately between 100 and 300 km in the plane perpendicular to the magnetic field.

[3] In this letter we address the transverse dimensions of chorus sources using simultaneous observations of intense chorus by four Cluster spacecraft localized close to the geomagnetic equator at a radial distance of 4.4 R_E . We analyze correlation of data from the four spacecraft at close separations. Our study is mainly based on high-resolution data of the wideband (WBD) wave instruments [*Gurnett et al.*, 2001]. We also use supporting data from the spectrum analyzers of the STAFF instruments [*Cornilleau-Wehrlin et al.*, 1997], the Whisper sounders [*Décrou et al.*, 2001], and spin-averaged measurements of the flux-gate magnetometers (FGM) [*Balogh et al.*, 2001]. In section 2 we present the observations, section 3 describes the correlation analysis, and, finally, in section 4 we summarize the results.

2. Observations of the Chorus Source Region

[4] During a perigee pass on April 18, 2002, the Cluster spacecraft were located on the night side (MLT of ≈ 2100) at a radial distance of 4.4 R_E . Global geomagnetic disturbances with the hourly equatorial Dst index below -120 nT at 0800 UT, and Kp index between 6- and 7o at 0000–0900 UT were accompanied by considerable irregular variations of the local magnetic field measured by the onboard FGM magnetometers. Intense chorus emissions were observed between 0820 and 0930 UT by the WBD wave instruments, by the STAFF-SA spectral analyzers, and by the Whisper relaxation sounders. The Whisper data give us an estimate of plasma frequency [P. Canu, private communication, 2002; *Canu et al.*, 2001] corresponding to the plasma density of a few particles per cm^3 . The cross-spectra of the electric and magnetic fluctuations below 4 kHz calculated by the STAFF-SA instruments indicate that the Poynting flux was directed southward at negative magnetic latitudes, and northward at positive magnetic latitudes, except in an interval of $\approx 4^\circ$ around the magnetic equatorial plane where the predominant direction fluctuates or cannot be determined. This narrow interval thus corresponds to the source region of chorus. Its location close to the equatorial plane was previously documented by *LeDocq et al.* [1998], and more recently from Cluster observations by *Parrot et al.* [2002]. The STAFF-SA data also show us that the average wave vectors were parallel to the magnetic field in the

¹Now at Faculty of Mathematics and Physics, Charles University, Prague, and at Institute of Atmospheric Physics, Czech Academy of Sciences, Prague, Czech Republic.

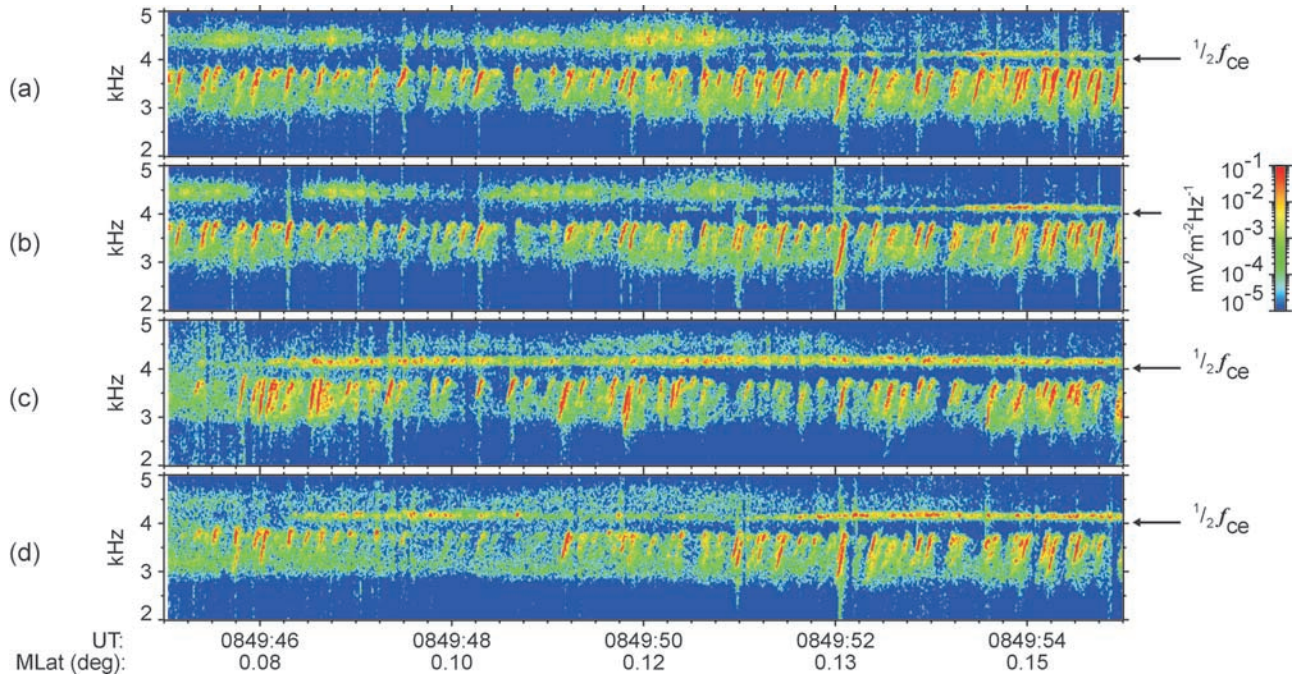


Figure 1. Detailed time-frequency power spectrograms of electric field fluctuations in the source region recorded by the WBD instruments on board the four Cluster spacecraft on April 18, 2002. Panels (a–d) show data from Cluster 1–4, respectively. Arrows indicate local $\frac{1}{2}f_{ce}$ for each spacecraft. Magnetic dipole latitude is given on the bottom for Cluster 1. Radial distance is $4.37 R_E$, and magnetic local time is 21.01 h during this interval.

source region, as previously observed, e.g., by Hayakawa *et al.* [1984].

[5] During the April 18th pass, the WBD instruments were set up to measure continuous waveforms with pass-band filters between 50 Hz and 9.5 kHz, and a sampling frequency of 27.44 kHz. The 90-m electric double-sphere antennas were used as sensors most of the time. The four spacecraft were located very close to each other. The maximum separation was 260 km along the field line and 100 km in the perpendicular plane. Assuming a characteristic plasma frequency of 12 kHz, and an electron cyclotron frequency of 8 kHz—as respectively obtained from the Whisper and FGM data in the source region—a typical parallel propagating wave at 3.5 kHz has a wavelength of approximately 30 km according to the cold plasma theory. The maximum perpendicular separation was thus only a few wavelengths. Figure 1 shows an example of electric field power spectrograms from the four Cluster spacecraft at time scales allowing us to see separate chorus elements below $\frac{1}{2}f_{ce}$. The four satellites surrounded the magnetic equator during this 10-s time interval, Cluster 1 being on the North of it, and the other three spacecraft being to the South. For example, at 0849:50 the magnetic latitudes were $+0.12^\circ$, -0.27° , -0.42° , -0.13° for Cluster 1–4, respectively. Just above $\frac{1}{2}f_{ce}$ we can identify intense narrow-band emissions similar to the observations of Muto *et al.* [1987]. Below $\frac{1}{2}f_{ce}$, we observe discrete chorus elements with power-spectral densities of more than $0.1 \text{ mV}^2 \text{ m}^{-2} \text{ Hz}^{-1}$, each of them rapidly rising in frequency with a slope of about 10 kHz/s. The spectrograms of Cluster 1 and 2 are very similar, and every chorus element seen by one of the spacecraft is seen on the other one. The spectrograms of Cluster 3 and 4 are more different but many common features are still seen on

the four spacecraft, for example, the intense element observed just after 0849:52.

3. Correlation Analysis

[6] In order to quantify the differences between the spectrograms observed in the chorus source region on the four spacecraft, we have analyzed their correlation. We have calculated averaged power-spectral densities in a 1-kHz band below $0.48 f_{ce}$, covering the distinct chorus elements seen, e.g., in Figure 1. For all the spacecraft we have used a common time resolution of 0.04 s, sufficient to distinguish the separate elements. This gave us 250 data points for each spacecraft in a 10-s time interval. We have then calculated the correlation of the common logarithms of these data for each pair of spacecraft, using the standard formulae for the Pearson's coefficient r of linear correlation, as well as the Spearman's rank correlation coefficient ρ and the two-sided significance levels P_ρ [Press *et al.*, 1992]. These last parameters P_ρ allow us to estimate the significance of the correlation results: the rank correlation is significant (ρ is significantly deviated from zero) if the probability P_ρ is small.

[7] In the input data, prior to the correlation analysis, the separate chorus elements appear as isolated peaks on the floor of background noise. The level of background noise in the source region is usually determined by the intensity of diffuse hiss-like waves observed in the same frequency range as discrete elements (see Figure 1 for an example), the level of the instrumental noise being by several orders of magnitude lower. The power-spectral density of the diffuse emissions is $\leq 10^{-4} \text{ mV}^2 \text{ m}^{-2} \text{ Hz}^{-1}$, while the discrete elements can reach the level of $1 \text{ mV}^2 \text{ m}^{-2} \text{ Hz}^{-1}$. Since

Table 1. Correlation analysis of chorus in Figure 1.

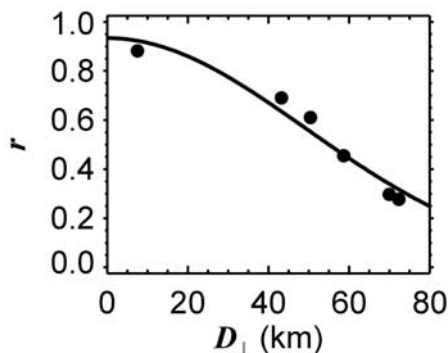
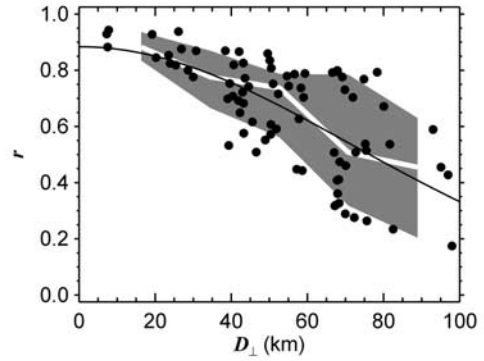
S/C	D_{\parallel}	D_{\perp}	r	ρ	P_{ρ}
1-2	187 km	7 km	0.88	0.87	$<10^{-38}$
1-3	258 km	72 km	0.28	0.30	10^{-6}
1-4	110 km	50 km	0.61	0.60	10^{-25}
2-3	70 km	69 km	0.30	0.32	10^{-7}
2-4	-77 km	43 km	0.69	0.70	10^{-37}
3-4	-148 km	58 km	0.45	0.47	10^{-15}

the background noise can influence the results we have tried to remove this influence prior to the correlation analysis. We have set all the input data which were below a predefined limit of $10^{-4} \text{ mV}^2 \text{ m}^{-2} \text{ Hz}^{-1}$ to this limit value itself, making a uniformly flat noise floor. The results, however, were always very close to the results obtained without that ‘noise flattening’ operation. We thus present only the results without that noise floor correction in the following.

[8] Table 1 summarizes the results of the correlation analysis in the time interval shown in Figure 1. Six different pairs among the four spacecraft are denoted in the left-most column. The separation distance D_{\parallel} is calculated as the component of the separation vector in the direction parallel to the ambient magnetic field, and the separation distance D_{\perp} is the modulus of the projection to the perpendicular plane. The results clearly show that both correlation coefficients r and ρ are ordered by D_{\perp} and not by D_{\parallel} . An estimate of standard deviation of r for uncorrelated data gives $\sigma_r \approx 0.06$, i.e., well below the r values obtained. The significance of the correlation is confirmed by the small values obtained for P_{ρ} . Figure 2 demonstrates that r approximately follows a gaussian function of D_{\perp} ,

$$r = A \exp\left(-\frac{D_{\perp}^2}{\Delta^2}\right) \quad (1)$$

A nonlinear least-squares fit of two free parameters, shown by solid line in Figure 2, gives us $A = 0.93$, $\Delta = 70 \text{ km}$. The result with $A < 1$ means that two spacecraft located along the same field line don’t record exactly the same data. There are, indeed, good reasons for slight differences. (a) The correlation is biased by modulation of the received power by the spacecraft spin motion which has a period of 4 s, and

**Figure 2.** Linear correlation coefficient for chorus emissions in Figure detail as a function of the perpendicular distance between the spacecraft. Fit of a gaussian function (see text) is plotted by solid line.**Figure 3.** Statistical analysis of r as a function of perpendicular separation. Shaded areas represent intervals between the 0.16-quantile and 0.84-quantile, white line in the middle showing the median (0.5-quantile) values. Fits of a gaussian function is plotted as in Figure 2.

inevitably different phases on each of the spacecraft; (b) Waveforms of intense elements are sometimes clipped by the finite dynamics of the instrument on at least one of the spacecraft; (c) Fluctuations of the magnetic field at spatial scales of D_{\parallel} could result a biased calculation of D_{\perp} - in this calculation we use the magnetic field vector averaged from all the four spacecraft; (d) Variations of wave properties with D_{\parallel} , although proven by our analysis not to be dominant can also decrease the correlation for small D_{\perp} .

[9] To obtain a more general idea on the structure of chorus emissions we have done similar analysis of the linear correlation coefficients for more data intervals recorded on April 18, 2002. Figure 3 shows results in 13 selected intervals of 10-s duration in the chorus source region, within the 4° interval of magnetic latitude around the equator. We have considered only those intervals, where distinct chorus elements were clearly defined, similarly as in Figure 1. We have excluded the data where the elements were so close to each other that it would be impossible to distinguish them in the frequency-integrated time series with the 0.04-s resolution. In each of the selected 13 intervals we have calculated the correlation coefficients for the 6 spacecraft pairs, giving the total number of 84 values for each coefficient. The results of the rank correlation (not shown) are similar to those of the linear correlation and the analysis gives us the same implications for the statistical significance of the results as has been demonstrated in the above example case. Similarly, there is no dependence of correlation coefficients on D_{\parallel} in the given interval of parallel separations. Although the values of r in Figure 3 are now much more scattered compared to Figure 2, the global trend of r decreasing with increasing D_{\perp} is still clearly seen. To demonstrate this trend, we have divided the total range of D_{\perp} into 5 equal subranges, i.e., from 0 to 20 km, from 20 to 40 km, etc. In each subrange we have calculated three quantiles of the corresponding subset of r values: the median value (i.e., the 0.5-quantile), the 0.16-quantile, and the 0.84-quantile. The last two quantiles correspond to estimates of values separated by one standard deviation from the mean value of a normal distribution. These parameters show how r globally varies with D_{\perp} and how the obtained values are scattered. We can see that the median

systematically decreases with D_{\perp} and that the results tend to be more scattered for higher D_{\perp} . When we use different lengths of the input data intervals ranging from 6 s to 20 s, i.e., both longer or shorter than 10 s, we obtain similar results for the three quantiles as shown in Figure 3. A nonlinear least-squares fit to the data in Figure 3 results in $A = 0.88$ and $\Delta = 101$ km (solid line).

4. Conclusions

[10] We have presented a correlation analysis of chorus observed in the source region by 4 closely separated spacecraft. Our principal conclusions are as follows. (a) Chorus elements below $\frac{1}{2}f_{ce}$ are significantly correlated at spatial separations up to 260 km along the field line, and up to 100 km in the perpendicular plane. (b) Within these limits, both the linear and rank correlation coefficients depend on the perpendicular separations and are independent on parallel separations. (c) The correlation coefficients decrease with perpendicular separation, approximately following a gaussian function with a half-width of 100 km. (d) The obtained characteristic scale is close to the general theoretical estimation by *Trakhtengerts* [1999]. Detailed comparison of these results with existing theories will be the subject of future work.

[11] **Acknowledgments.** Many thanks are due to J. Pickett, Science Data Manager of the WBD instrument, who helped us with the data and took care of the operations, to R. Huff, Project Manager, who did the WBD calibration, and to J. Dowell, J. Seiberger, and R. Brechwald who prepared the preprocessing software. We thank P. Canu and P. Décr  au (PI of Whisper) for useful information on the Whisper data. We acknowledge discussions on the STAFF-SA data with N. Cornilleu-Wehrin (PI of the STAFF experiment), M. Parrot, M. Maksimovic, and C. Harvey, and we thank A. Balogh (PI of the FGM magnetic field experiment) for access to the spin-resolution magnetic field data used for reference. Provisional Dst index was obtained from WDC-C2, Kyoto University. This work was supported by the NASA Goddard Space Flight Center under Grant No. NAG5-9974. O. Santol  k acknowledges additional support from grants ME 467, MSM 113200004, and GACR 205/02/0947.

References

- Balogh, A., et al., The Cluster Magnetic Field Investigation: Overview of in-flight performance and initial results, *Ann. Geophys.*, *19*, 1207–1217, 2001.
- Canu, P., et al., Identification of natural plasma emissions observed close to the plasmapause by the Cluster-Whisper relaxation sounder, *Ann. Geophys.*, *19*, 1697–1709, 2001.
- Cornilleu-Wehrin, N., et al., The Cluster spatio-temporal analysis of field fluctuations (STAFF) experiment, *Space Sci. Rev.*, *79*, 107–136, 1997.
- D  cr  au, P. M. E., Early results from the Whisper instrument on Cluster: An overview, *Ann. Geophys.*, *19*, 1241–1258, 2001.
- Gurnett, D. A., et al., First results from the Cluster wideband plasma wave investigation, *Ann. Geophys.*, *19*, 1259–1272, 2001.
- Hayakawa, M., Y. Yamanaka, M. Parrot, and F. Lefeuvre, The wave normals of magnetospheric chorus emissions observed on board GEOS 2, *J. Geophys. Res.*, *89*, 2811–2821, 1984.
- Helliwell, R. A., A theory of discrete emissions from the magnetosphere, *J. Geophys. Res.*, *72*, 4773–4790, 1967.
- Lauben, D. S., U. S. Inan, T. F. Bell, D. L. Kirchner, G. B. Hospodarsky, and J. S. Pickett, VLF chorus emissions observed by Polar during the January 10, 1997 magnetic cloud, *Geophys. Res. Lett.*, *25*, 2995–2998, 1998.
- LeDocq, M. J., D. A. Gurnett, and G. B. Hospodarsky, Chorus source locations from VLF Poynting flux measurements with the Polar spacecraft, *Geophys. Res. Lett.*, *25*, 4063–4066, 1998.
- Muto, H., M. Hayakawa, M. Parrot, and F. Lefeuvre, Direction finding of half-gyrofrequency VLF emissions in the off-equatorial region of the magnetosphere and their generation and propagation, *J. Geophys. Res.*, *92*, 7538–7550, 1987.
- Omura, Y., D. Nunn, H. Matsumoto, and M. J. Rycroft, A review of observational, theoretical and numerical studies of VLF triggered emissions, *J. Atmos. and Terr. Phys.*, *53*, 351–368, 1991.
- Parrot, M., O. Santol  k, N. Cornilleu-Wehrin, M. Maksimovic, and C. Harvey, Source location of chorus emissions observed by CLUSTER, submitted to, *Ann. Geophys.*, 2002.
- Press, W. H., B. P. Flannery, S. A. Teukolsky, and W. T. Vetterling, *Numerical Recipes*, Cambridge Univ. Press, New York, 1992.
- Sazhin, S. S., and M. Hayakawa, Magnetospheric chorus emissions: A review, *Planet. Space Sci.*, *40*, 681–697, 1992.
- Trakhtengerts, V. Y., A generation mechanism for chorus emission, *Ann. Geophys.*, *17*, 95–100, 1999.

O. Santol  k, Faculty of Mathematics and Physics, Charles University, V Hole  vov  k  ch 2, CZ-18000 Praha 8, Czech Republic. (ondrej.santolik@mff.cuni.cz)

D. A. Gurnett, Department of Physics and Astronomy, University of Iowa, Iowa City, IA 52242-1479, U.S.A. (gurnett@space.physics.uiowa.edu)